

# Hillslope and channel evolution in a marine terraced landscape, Santa Cruz, California

Nan A. Rosenbloom<sup>1</sup> and Robert S. Anderson

Department of Earth Sciences and Institute for Tectonics, University of California, Santa Cruz

**Abstract.** A flight of marine terraces along the central California coastline provides a unique setting for the study of topographic evolution. Wavecut platforms mantled by 2-6 m of marine terrace cover deposits are separated by 10-50 m tall decaying sea cliffs. Paleocliff edges become more rounded with age, yet the details of the profiles and frequent bedrock exposure on the upper slopes imply weathering-limited transport. Five bedrock stream channels etched through the marine terrace sequence display one to three distinct convexities in their longitudinal profiles. Detailed hand level surveys of the hillslopes and of the stream channel longitudinal profiles constrain hillslope evolution and channel incision components of a numerical model of landscape evolution. We account for regolith production as a function of regolith depth. In accord with the field observation that hillslope processes are presently dominated by the activities of burrowing rodents, the transport process is taken to be diffusive. Stream incision is assumed to be controlled by stream power, for which we use the surrogate of local drainage area-slope product. Best fits of the numerical model to field data imply: hillslope diffusivity is  $10 \text{ m}^2 \text{ kyr}^{-1}$ ; regolith production rate on bare bedrock is  $0.3 \text{ m kyr}^{-1}$ , and falls off rapidly with regolith cover; and the constant controlling the efficiency of stream incision is  $5 \text{ to } 7 \times 10^{-7} \text{ m}^{-1} \text{ kyr}^{-1}$ .

## Introduction

The study of large scale landscape evolution requires an understanding of the linkage between small scale channels and hillslopes, as well as constraint on the tectonically driven source of long-wavelength topography. Testing and verification of existing landscape evolution models typically founder on the difficulties of establishing timing in the landscape and on the absence of information about the initial conditions for geomorphic features. Meaningful rates of erosion at timescales relevant to large scale landscape evolution are therefore rare. Most rates are derived from basin-integrated measures such as reservoir sedimentation rates or from point measurements such as those derived from concentrations of in situ produced cosmogenic radionuclides [e.g., *Nishiizumi et al.*, 1993]. Neither yield information about the geometric evolution of particular landform elements.

The marine terraced landscape is a simple one in which initial conditions, final (present) form, and age of different geomorphic elements is constrained. It therefore provides information sufficient to determine the process rates that lead to the evolution of both hillslopes and channels at the tectonically active margins of a continent. Marine terraces form along uplifting coastlines subjected to periodic large-scale fluctuations in sea level. Surf attack causes the backwearing of vertical cliffs and simultaneous downwearing of the subjacent wavecut platform. These notches are most efficiently cut into the landscape when the waves impact the

coastline at the same location year after year, which occurs when the relative rise of the land and of the sea are nearly equal. This condition exists both just after sea level lowstands and just prior to sea level highstands [*Bradley and Griggs*, 1976]. The lowstand platforms are subsequently drowned during sea level rise. The highstand platforms are abandoned upon sea level drop and may achieve significant altitude by the time of subsequent sea level highstands, to be preserved as separate terraces. During sea level retreat from the abandoned sea cliff, a thin, several meter thick terrace cover deposits of marine sands accumulates on the abrasional platform.

The abrasional platforms tend to be crudely planar, with relatively low roughness, and are backed by straight to sinuous sea cliffs. These planar surfaces, thinly mantled by the terrace sands, form broad, low interfluvial stream channels etched through the landscape. This landscape may be characterized by two types of hillslopes, each with a different lower boundary condition. The ancient sea cliffs are bounded by the next lower terrace platform, where the products of cliff decay accumulate. These hillslopes are essentially two-dimensional, making analysis of their evolution uncomplicated by convergence and divergence of material from out of the profile. The streams crossing the terraced fringe of the landscape provide a second lower boundary condition in which slope debris is continuously removed and base level is lowered. These streams flow in bedrock channels incising into the uplifting rock mass and are continuously adjusting to a fluctuating sea level. Their profiles should reflect the interaction of erosive and tectonic processes.

That the marine terrace setting is appropriate for the study of landscape evolution has been recognized by earlier workers [*Hanks et al.*, 1984], who used a coast-normal profile of the flight of Santa Cruz marine terraces to estimate topographic diffusivities on the two-dimensional decaying sea cliffs. They argued that linear diffusion is an appropriate first-order model. More recent work has emphasized the importance of

<sup>1</sup>Now at Department of Geological Sciences, University of Colorado, Boulder.

Copyright 1994 by the American Geophysical Union.

Paper number 94JB00048.  
0148-0227/94/94JB-00048\$05.00.

incorporating the rate at which bedrock is transformed into transportable debris through weathering processes [e.g., *Anderson and Humphrey, 1989*]. Our use here of observations of regolith thickness in conjunction with detailed topographic profiles is intended to provide constraint on both regolith production and transport process rates.

Recent work on large scale landscape evolution [e.g., *Koons, 1989*] has reemphasized the importance of the role played by channels in the geomorphic system. As they set the lower boundary condition for the adjacent slopes, their incision rates can greatly influence the total denudation rate in the landscape. While much work has addressed the response of

alluvial channels to changing base levels [e.g., *Begin, 1988*], very little is known about the process styles and rates in bedrock channels, which are the most important in rapidly uplifting terrains. The response times of bedrock channels are long, meaning that information about the processes and their rates is scarce. The principal exceptions are badland channels [e.g., *Howard and Kerby, 1983*], where the response times are indeed quite short because of the weak lithologies, and more recent work in the coastal streams of California [*Seidl and Deitrich, 1992*] and of Hawaii (*M. A. Seidl et al., manuscript in preparation, 1994*), where new techniques using cosmogenic radionuclides allow timing to be established.

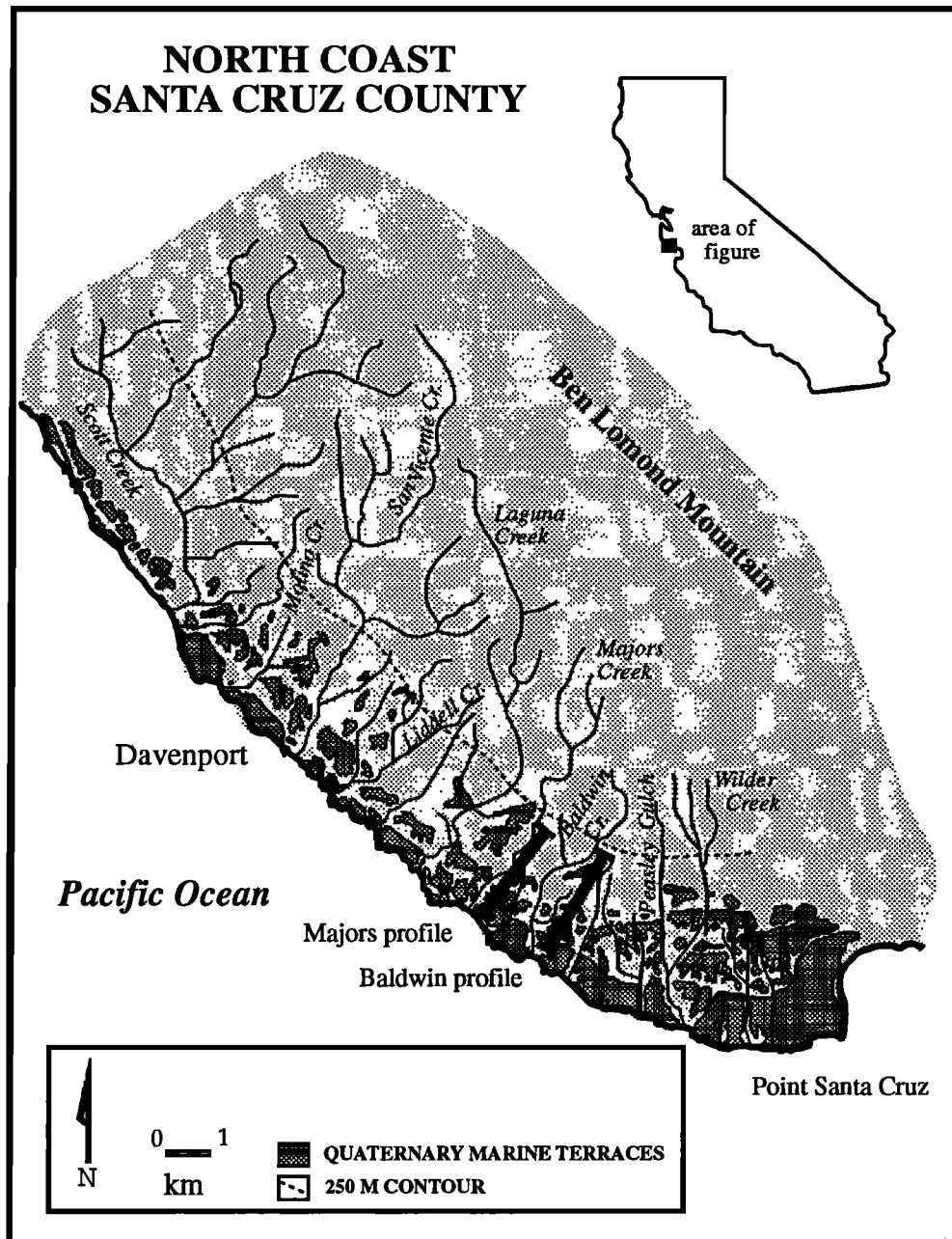


Figure 1. Coastline north of Santa Cruz, California. Several streams are shown crossing the fringe of the landscape dominated by several marine terraces. Throughgoing streams cutting the entire terrace sequence have source areas above 250 m altitude, shown roughly as the dotted line. Terrace riser profiles 1 and 2 used as constraints in the numerical model are also shown.

Chappell [1974], working in the coral terraces of the Huon Peninsula, Papua New Guinea, is the first to have used the profiles of channels to constrain bedrock channel process types and rates making use of the time constraints inferred from the ages of these spectacular terraces. His work was confined to the smallest of channels that have evolved within the terrace sequence.

Our goal is to use profiles from this well-timed and geometrically tractable landscape to assess geomorphic processes and to calibrate long-term rates using a landscape evolution model with both hillslope and channel components. The results can then be used both to construct models of landscape evolution that are larger in scale, for instance, of the evolution of the Santa Cruz Mountains as a whole [Anderson, 1990; this issue], and to develop insight into the evolution of marine terraced landscapes in general.

### Geologic Setting

A well-preserved flight of at least five emergent marine terraces graces the 30 km of coastline north of Monterey Bay, California, between Santa Cruz and Greyhound Rock (Figure 1). We focus on a 5-km reach of coast north of Santa Cruz where the terrace morphology is particularly well preserved. The study area lies within a complex region traversed by numerous faults that together comprise the crustal North American-Pacific plate boundary. Parts of the region are slowly deforming as a result of uplift related to advection of crust around a restraining bend on the San Andreas fault to the northeast [Anderson, 1990, this issue]. Uplift rates along the

coast vary from 0.16 to 0.48 m kyr<sup>-1</sup> [Bradley and Griggs, 1976], while those in the study area are roughly 0.3 m kyr<sup>-1</sup>. Uplift mechanisms along the study reach include coseismic uplift associated both with a reverse component of slip on the steeply SW dipping Loma Prieta fault in the restraining bend of the San Andreas fault 20-30 km inland (see Figure 2) and with a small component of reverse slip on the steeply SE dipping San Gregorio fault 5-10 km offshore [Anderson and Menking, 1994].

The marine terraces are etched into the side of Ben Lomond Mountain, a SW tilted crustal block whose long axis parallels the coast north of Santa Cruz (see Figure 3). Erosion of the block has exposed a crystalline core of Paleozoic metasedimentary and Mesozoic plutonic rocks similar to those seen in other parts of the Salinian block [Leo, 1967; James, 1992]. This crystalline complex is unconformably overlain by gently southwest dipping Tertiary marine sediments [Clark, 1981]. It is into these Tertiary sediments, primarily the Santa Cruz Mudstone, a hard, medium- to thick-bedded, pervasively jointed siliceous organic mudstone of late Miocene age [Clark, 1981], that the marine terraces are cut. The durability and low solubility of the Santa Cruz Mudstone are primarily responsible for the excellent preservation of the marine terraces along this reach of the coast.

The underlying strata are relevant solely to the streams that incise most deeply into the terraced landscape. Immediately beneath the Santa Cruz Mudstone lies the very thick-bedded, friable Santa Margarita Sandstone, below which is the sandy siltstone and siliceous mudstone of the Monterey Formation. The lowest stratigraphic unit exposed in the marine terraced

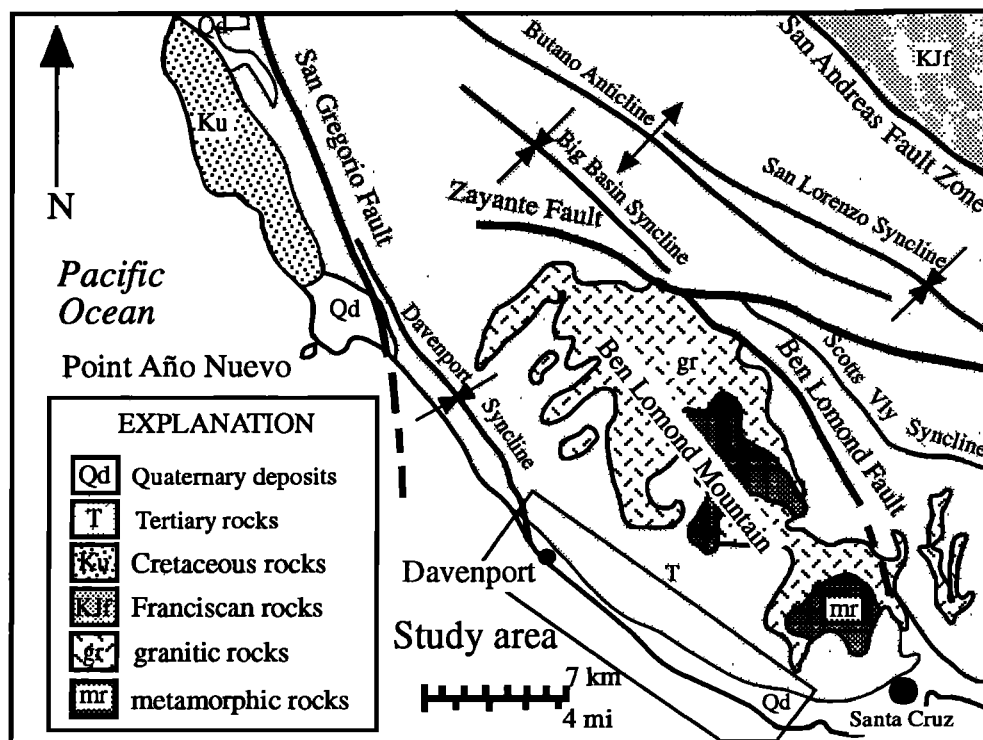


Figure 2. Geological map of coastal California north of Santa Cruz. Study area (box) geology dominated by gently seaward tilted Tertiary sediments overlain by thin Quaternary marine terrace deposits. The mountain massif into which the terraces are etched is controlled by the Cretaceous Salinian Block Ben Lomond Complex. Folding becomes more intense nearer the San Andreas fault zone approximately 30 km NE of the study site.



**Figure 3.** Aerial photograph of the marine terraced landscape showing the present platform and inner edge, and several raised platforms backed by decaying cliffs. The farther back into the landscape one looks, the more difficult it is to recognize old platforms, in part due to decay of the cliffs, but largely due to incision of the terraced landscape by numerous tributaries of through-cutting channels.

landscape is quartz diorite-granodiorite of the crystalline complex of Ben Lomond Mountain [Clark, 1981; James, 1992].

The Santa Cruz marine terraces have been mapped by many workers including Lawson [1893], Wilson [1907], Branner *et al.* [1909], Rode [1930], Page and Holmes [1945], Alexander [1953], Bradley [1956, 1957, 1965], Bradley and Addicott [1968], Clark [1966, 1970], Jahns and Hamilton [1971], and Lajoie *et al.* [1972, 1986]. Bradley and Griggs [1976], whose terminology we adopt, mapped and correlated the terrace

sequences, identifying inner edge locations from known terrace inner edge exposures, interpolation of terrace profiles, and hammer seismic surveys. Much of the more recent work has been motivated by the desire to detail the spatial and temporal distribution of uplift along this reach of coast [Bradley and Griggs, 1976; Anderson, 1990; Valensise and Ward, 1991; Anderson and Menking, 1994].

Absolute dating of the Santa Cruz marine terraces has proven difficult owing to a paucity of fossil assemblages that include appropriate coral species. There is continuing debate

**Table 1.** Platform Names, Inner Edge Ages, Distances From the Modern Coastline, and Initial Cliff Heights Used in the Numerical Model

Terrace	Age*, ka (Isotope Stage)		Formation Altitude†, m	Distance From Modern Seacliff, m	Initial Cliff Height, m	
	Hanks <i>et al.</i>	Lajoie <i>et al.</i>				
Highway 1	105 [5c]	125	-1 to -4	(-9)	650	53
Western	212 [7]	430	0 to +1	(-7)	1150	50
Wilder	330 [9]	800	0	(+4)	1625	40
Blackrock	500 [13]	900-1000	0	0	2075	20
Quarry	610 [15]	1100-1300	0	0	2375	20

See Figure 4.

\*Preferred age assignments and isotope stages based upon Hanks *et al.* [1984] adjusted for more recent sea level curves [Chappell and Shackleton, 1986], and alternative age assignments favored by Lajoie *et al.* [1986].

†Rockwell *et al.* [1992] and T. Rockwell (personal communication, 1993); numbers in parentheses based upon Huon Peninsula sea level curve of Chappell [1983]. Zero altitudes are used when no other constraint is available.

over the assigned ages of the terraces and their correlation with global sea level curves. The lowest emergent terrace, Highway 1, has a U series date of 68,000 to 100,000 years B.P. [Bradley and Addicott, 1968] and an amino-acid date of  $130,000 \pm 50,000$  years B.P. [Lajoie et al., 1975]. The older, higher terraces have been dated solely through correlation techniques based upon detailed  $\delta^{18}\text{O}$  sea level curves and an assumed constant uplift rate [Bradley and Griggs, 1976; Hanks et al., 1984]. Two possible correlations for Highway 1 terrace of 105 ka and 125 ka unfortunately appear to be equally well supported by the terrace altitude data [Anderson and Menking, 1994], although we favor the 5c (105 ka) age for the Highway 1 platform. We use the terminology and age correlations listed in Table 1.

## Climate and Vegetation

The region experiences a Mediterranean climate with mild summers and cool, rainy winters. Ninety percent of the highly variable annual precipitation falls between November and March. Orographic effects from the Santa Cruz Mountains result in pronounced variations in regional precipitation such that the terraces along the coast receive considerably less rainfall (50-76 cm annually) than the higher slopes of Ben Lomond Mountain (>150 cm) [Rantz, 1968].

Recent assessment of an ensemble of paleoclimatic indicators throughout the United States, combined with a global circulation modeling effort [Anderson et al., 1988], leads to the hypothesis that the late glacial climate at this latitude in the American West was dominated by the southward deflection of the mean annual position of the jet stream, with its associated high precipitation. More locally, paleoclimatic indicators from coastal California imply climate fluctuations in phase with North American glaciations throughout the Pleistocene [Sims et al., 1981; Johnson, 1977]. While glacial and interglacial conditions represent periods of climatic extremes, the majority of the Pleistocene was characterized by intermediate climatic conditions [Porter, 1989]. In this region, the late Pleistocene climatic fluctuations appear to have been minor. Geologic, pedologic, and paleobotanical evidence indicates that coastal California experienced a semiarid Mediterranean climate throughout the Late Pleistocene with glacial periods characterized by only moderately cooler, wetter conditions expressed in greater seasonal precipitation contrasts and a greater frequency of high-intensity winter storm events [Johnson, 1977; Gorsline et al., 1976; Sims et al., 1981]. In the calculations carried out below, we therefore assume that the geomorphically important components of the climate of coastal California have remained relatively constant throughout the lifetime of the landscape we are considering (<0.5 M.y.), and that the geomorphic process types and their rates have been likewise steady.

The two prominent lower terraces are currently farmed, while the unplowed upper marine terraces are covered with native and introduced grasses (see Figure 3). The upper meadows of the highest identified terrace merge with redwood forests that continue to the crest of Ben Lomond Mountain. Redwood, oak, and madrone forests dominate both the upper basins and the cool, wet lower reaches of the larger stream channels crossing the marine terraces. It is thought that redwood forests never covered the terrace surfaces, even during wetter climates. It is therefore likely that the present coastal vegetation is approximately that of the past and that variation

in geomorphic rates result primarily from changes in the statistics of rain-delivering storms.

## Landscape Description

### Wavecut Platforms

During glacial periods, eustatic sea level is estimated to have dropped by 150 m [Fairbanks, 1989], placing glacial coastlines more than 5 km seaward of the present shoreline along the Santa Cruz coast. While the mean tectonic uplift rate deduced from the Santa Cruz terraces is a fraction of  $1 \text{ mm yr}^{-1}$  [e.g., Bradley and Griggs, 1976; Anderson and Menking, 1994], sea level changes associated with the transition from glacial to interglacial stages are inferred to have reached  $30 \text{ mm yr}^{-1}$  [Bard et al., 1990; Fairbanks, 1989]. It is therefore safe to assume that the majority of the incision of the sea cliffs and the associated abrasion of the subjacent wavecut platforms was nearly coincident with the sea level high and lowstands. Only then would rates of sea level change have roughly equaled the low tectonic uplift rates.

Clearly, later more extensive terrace cutting events may erase the record of previous sea level highstands, making the problem analogous to that of moraine survival [Gibbons et al., 1984]. While sea level has risen and fallen numerous times throughout the Pleistocene, relatively few sea level maxima are preserved as marine terrace platforms. Once a sea cliff is abandoned, it will be preserved unless a subsequent sea level highstand (1) is higher than the tectonic uplift accomplished between successive highstands or (2) lasts long enough to allow retreat of the active cliff beyond the position of the next highest abandoned sea cliff. Although the terrace record of a sea level highstand may be erased by this latter mechanism, we argue below that the profiles of appropriate streams may still preserve a record of the earlier highstand.

Rates of cliff retreat measured from aerial photographs between 1930 and 1980 vary from 0.0 to  $0.2 \text{ m yr}^{-1}$  north of Santa Cruz [Best and Griggs, 1991]. Although cliff retreat is not a process we attempt to explain or to model in the present work, these rates are significantly greater than any other local geomorphic rates.

The modern wavecut platform "tread" is a  $0.5\text{-}2.0^\circ$  slope projecting seaward from the active sea cliff [Bradley and Griggs, 1976]. The platform bedrock topography is relatively planar, with surface roughness of 2-4 m. The emergent terrace surfaces are even more planar than the underlying wavecut platforms, owing to the regolith mantle. These terrace cover deposits consist of 1-4 m of poorly consolidated sands and gravels deposited during sea level recession [Bradley, 1957], overlain spottily by eolian deposits and by colluvium at the back edges of the terraces (Figure 4). Apart from the burrowing activity of animals, regolith of the terrace treads appears to be relatively stable, a function of the low slope angle ( $1\text{-}2^\circ$ ) and the complete vegetative cover. Analysis of the terrace soils reveals that the most significant weathering occurs within the upper 60 cm of the terrace deposit cover. A 30 to 60 cm thick black loamy soil is produced primarily from the chemical and physical breakdown of the sandy beach deposit (Figure 4). Apart from the effects of in situ weathering, the deposits are mineralogically uniform with depth [Bradley, 1957]. Artificially cleared surfaces of wavecut platforms more than 100 kyr in age reveal intact pholad borings, reinforcing the inference that there is negligible bedrock weathering under typical terrace cover deposits.

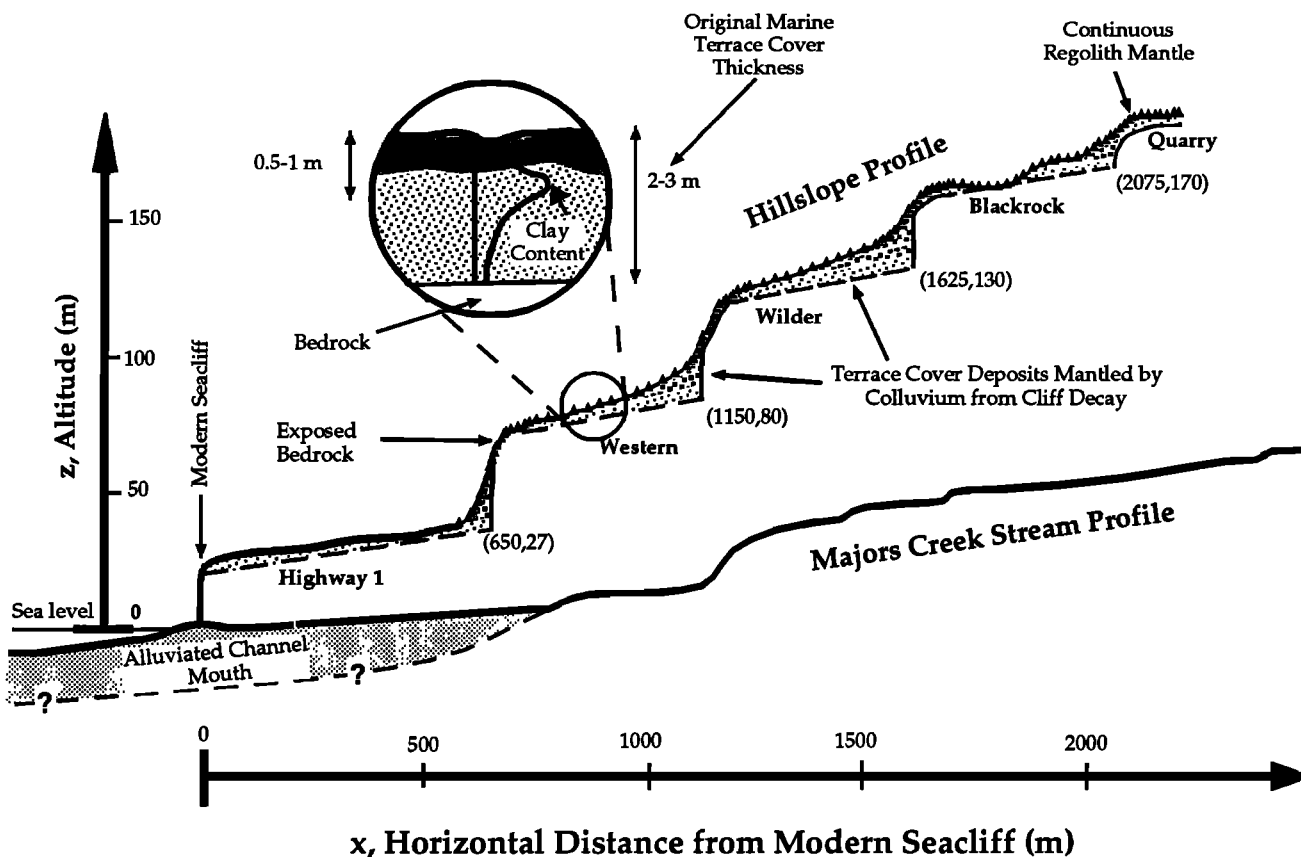


**Figure 4.** Combined terrace slope and stream profile hand-leveling data for Majors Creek and adjacent interfluvium. Terrace cover consists of original several meter thick marine regressive sands overlain by colluvium from sea cliff decay. A dark organic soil is well-expressed in the top 1 m of the regolith, with clay content peaking at roughly 0.5 m depth. Weathering of bedrock beneath this cover deposit is minimal. Patches of bedrock are exposed in the tops of the youngest paleocliffs, while older cliff tops display continuous regolith cover. The inferred altitudes and horizontal distances from the present shoreline are denoted for all inner edges. In the stream profile, note the convexities shown in less detail. The lowest reach of the channel is alluviated, corresponding to the drowning of the mouth of this and other similarly sized creeks upon deglaciation-induced sea level rise. Bedrock is at least 20 m below present sea level at the coast.

### Hillslopes

The initially vertically sea cliffs decay dramatically with time. Cliff-normal topographic profiles display maximum slopes that diminish with increasing cliff age, prompting the diffusional characterization of the surface processes by *Hanks et al.* [1984]. However, hand-level surveys taken at two locations roughly 1.5 km apart, and spanning the complete sequence of emergent terraces (Figure 5), reveal that the pale-cliff profiles are not perfectly symmetrical. The convex-up top of the cliff displays a shorter radius of curvature than the concave-up deposit at its base. Observations of bedrock outcroppings during surveying, as well as cross sections through the cliff exposed by stream incision reveal extremely thin to nonexistent regolith cover over the top half of the cliff. Together, these observations imply that the asymmetry may be due to a weathering-limited hillslope system, as discussed by *Anderson and Humphrey* [1989].

The main transport process acting on these grassy hillslopes at present is due to the burrowing activity of rodents, primarily the ground squirrel (*Spermophilus beecheyi*) and the mole (*Thomomys thomomys*). This process may be considered diffusive in that the transport rate is

dependent linearly on local slope [see *Rosenbloom*, 1992], with the rate constant dependent on such measurable quantities as mound volumes, burrowing intensity (number of burrows per unit area), and mean offsets of mounds from burrow mouths.

### Channels

As in other settings, channel dissection of the terraces increases with increasing terrace age [*Verma*, 1973; *Chappell*, 1974]. Wide, young platforms give way to narrower platforms higher in the sequence, and finally merge into ridge and valley morphology typical of the remainder of the Santa Cruz Mountains above the highest recognizable platform (Figure 3). The timescale over which recognizable platforms are preserved depends on the initial channel spacing, on the incision rates of the channels, and on the evolution of hillslopes adjacent to the channel walls.

The section of the coastline from Big Sur north to Half Moon Bay is dominated by drainages of three different scales: large drainage basin streams, intermediate streams that flow through the terrace sequence, and small streams with drainage areas internal to the terrace sequence. With the exception of

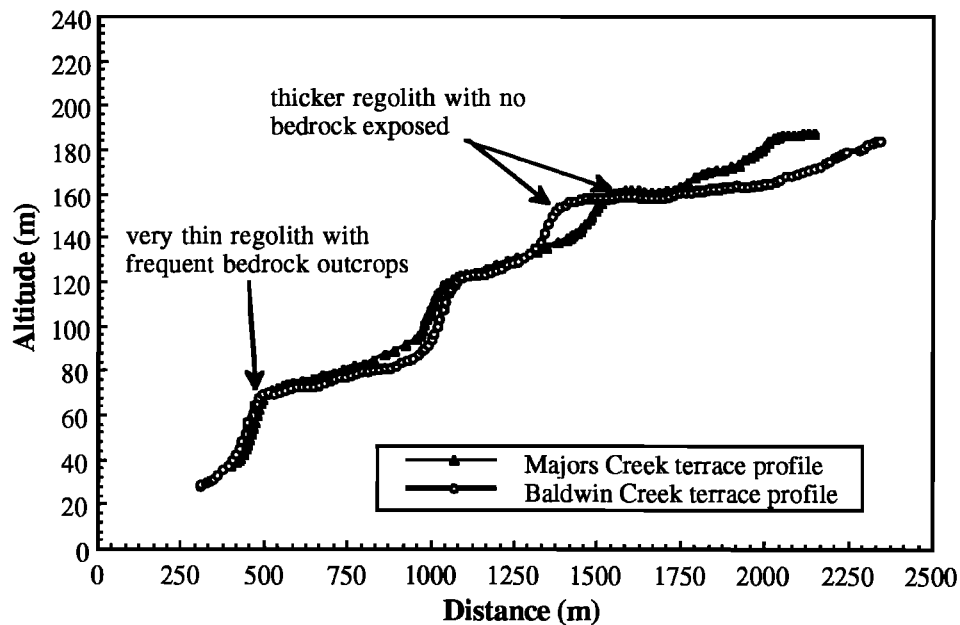


**Figure 5.** Two hand-leveled profiles of marine terrace surfaces measured on interfluvies depicted in Figure 1 (one of these profiles is also shown in Figure 4), demonstrating close similarity of altitudinal patterns. Note the coincidence of the inferred altitudes of the inner edges. The slight differences in the horizontal position of the paleocliffs, and hence in platform width, are due to variations in the rates of sea cliff retreat along the coast. The decayed cliffs show remarkable similarity in form, the youngest (lowest) cliffs showing sharpest convexities, while the oldest show more diffuse upper edges. Note also the asymmetry, produced by the sharper, high curvature convex tops and the lower curvature concave bases of the decayed cliffs, a detail more apparent in these high-density surveys. Upper reaches of young cliffs commonly display bedrock patches, while older cliff edges show little bedrock and generally thicker regolith cover.

Scott and Waddell Creeks, all of the largest streams (basin areas  $>50 \text{ km}^2$ ) lie south of Point Santa Cruz within Monterey Bay. These large streams have relatively smooth longitudinal profiles, with channel slopes decaying monotonically from the headwaters to the coast. Their mouths are alluviated.

The streams incising the Quaternary marine terraces within the study area fall into the two smaller stream categories: five to six throughflowing streams that drain altitudes above 250 m; and seven shorter streams that arise completely within the marine terrace sequence. The shorter streams have small drainage areas and are all ephemeral. They terminate in small alluvial fans at the base of the paleosea cliffs. The drainage basins of throughflowing streams are of order  $10\text{--}20 \text{ km}^2$  and tap regions of slightly higher rainfall on the coastward flank of Ben Lomond Mountain. The bulk of each of these basins lies above the terraced landscape. The lower-order tributaries to these streams are ephemeral, while channel flow in the main stem is generally maintained year-round from spring and groundwater discharge. Through the terrace sequence, the channels are narrow and straight, deeply incised, with steep,  $30\text{--}48^\circ$  channel walls (see Figure 3). The mouths of these streams are universally alluviated.

Bedrock is exposed along the length of the stream channels except where slope failures have introduced large amounts of debris or at the drowned channel mouths at altitudes close to sea level. In places, the Santa Cruz Mudstone is eroded through, exposing the Lompico Sandstone or Salinian block quartz diorite [Clark, 1981; James, 1992]. We found neither fill nor strath fluvial terraces. Cobbles and boulders within the channels consist primarily of Ben Lomond granites and

quartz diorite from the Salinian block complex. Channel alluvium varies from coarse sand and gravel to fine silt and mud. Many of the bedrock reaches are deeply incised by polished, sinuous, narrow channels, suggesting that abrasion by transported particles is an important erosion mechanism in these streams. While a siliceous cement impedes dissolution of the Santa Cruz Mudstone, stream sections through the calcareous Lompico Sandstone display numerous karstlike dissolution cavities in the channel bedrock. Large- and small-scale landsliding of the hillslopes bordering the channels temporarily dam or partially obstructs channel drainage. However, most channels are presently unobstructed by debris, indicating that landslides pose only short-term barriers to channel incision.

The throughgoing streams display two to three prominent convexities, as measured from U.S. Geological Survey (USGS) topographic maps (Figure 6). More detail is seen in a hand level survey of Majors Creek (see Figure 4 and 10). The convexities range from 10 to 55 m high and 90 to 580 m long, with typical gradients of  $3.0\text{--}7.5^\circ$ . Stream gradients between convexities are roughly  $1\text{--}2^\circ$ . The convexities at higher altitudes in the profiles appear to be more subtle than their lower-altitude counterparts. The convexities occur in several lithologies, including Santa Margarita Sandstone (Liddell Creek), Lompico Sandstone (Laguna, Baldwin), and quartz diorite (Majors Creek). The lowest stream convexity, roughly corresponding with the altitude of the first emergent marine terrace inner edge, coincides with a change in channel lithology from Quaternary alluvium to bedrock, i.e., the channel mouths were drowned by the modern sea level highstand.

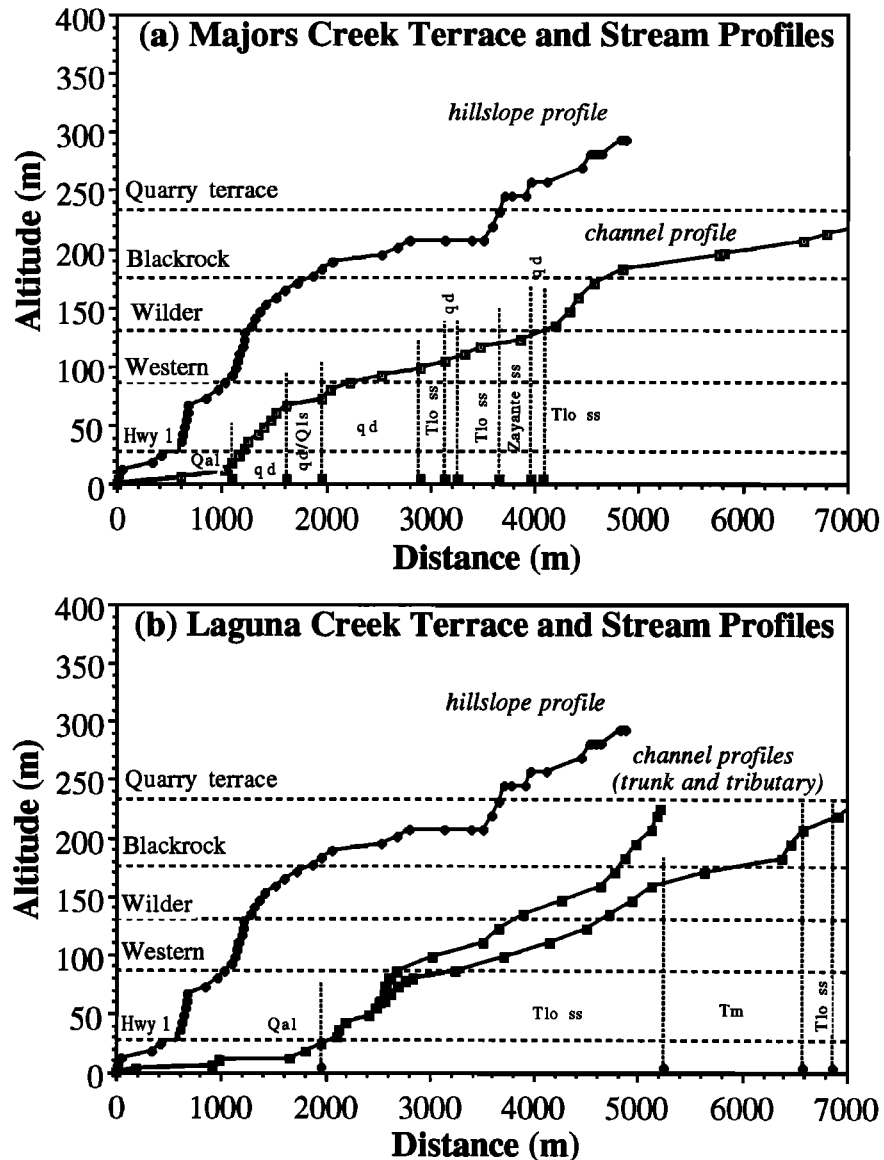


**Figure 6.** Profiles of the marine terrace surfaces and adjacent streams incising them, taken from U.S. Geological Survey topographic quadrangles at 20-40 foot (6-12 m) contours. (a) Majors Creek; (b) Laguna Creek; (c) Baldwin Creek; (d) Wilder Creek and Peasley Gulch. Also shown are the generalized altitudes of the five main marine terraces (horizontal lines) and lithologic boundaries from the geologic map (vertical lines). In each terrace profile, the steps associated with the marine platforms are clear; older higher paleocliffs are consistently more rounded. The stream profiles, including major tributaries in three of the four cases, show several prominent convexities that appear to correlate with terrace platforms. No clear association may be made between lithologic boundaries and the location of these convexities. Note that the shorter tributaries enter the trunk stream with higher slopes, as required by *Seidl and Dietrich's* [1992] stream power argument for channel incision.

All but two of the stream convexities occur within a single lithology, relatively far from the nearest lithologic boundary. Long profiles of the stream channels do not indicate a correlation between landslide features and channel convexities. These observations, together with coast-normal geologic cross sections [Clark, 1981; Brabb, 1989], suggest that convexities do not appear to be associated with, or to be limited to, any particular channel lithology, or to changes in lithology.

Offshore side-scan sonar data indicate that bedrock channels of the intermediate size streams along the north coast,

including Majors, Laguna, Baldwin, and Wilder Creeks, continue as sand-filled troughs seaward across the modern wavecut platform, indicating that they predate the present sea level highstand. Using data from water well logs drilled in alluvial fill near the mouth of Laguna Creek and assuming a channel gradient of  $1.5^\circ$ , we estimate that the elevation of the bedrock channel of Laguna Creek may be significantly greater than 15 m below sea level at the coast.

The throughflowing streams are therefore incised antecedent drainages continually responding to base level changes driven by both tectonic uplift and glacially induced sea level swings.

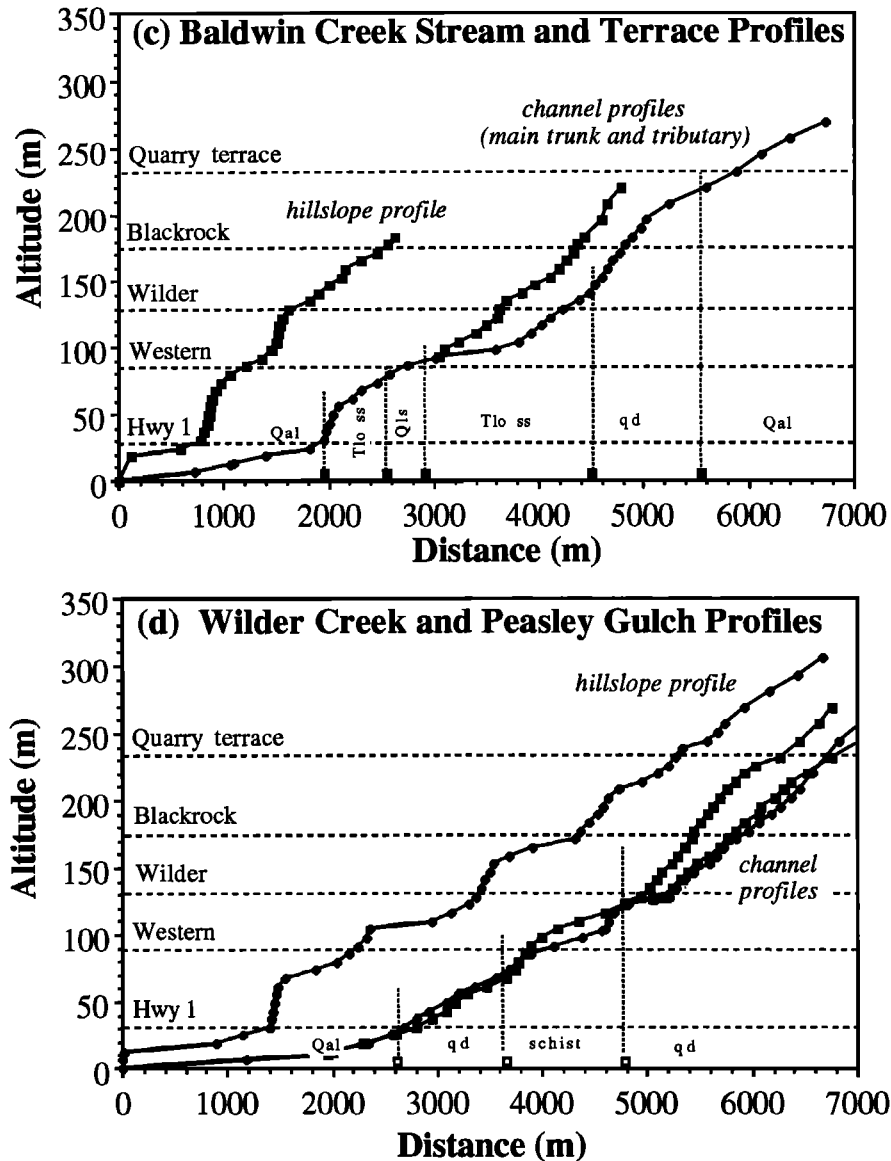


Figure 6. (continued)

As the larger streams on the north coast, Scott and Waddell Creeks, do not display prominent convexities in their lower sections, it appears that the size of the stream is important in the creation and preservation of channel convexities. High stream power may erase channel convexities or, as we will argue, may control whether a convexity will form in the first place.

### Derivation of the Model Rule Set

#### Terrace Platform Rules

Our model does not include a wavecut platform/sea cliff retreat process rule. Instead, we place marine terraces in the model at the appropriate times and altitudes determined by our correlations to the assumed sea level curve and at horizontal distances relative to the present sea cliff determined from the hand level surveys. Wavecut platforms and associated sea cliffs are therefore created instantaneously at the assumed time of the associated sea level highstand, an assumption motivated by the fact that cliff retreat is the fastest

geomorphic process acting. The entire topography is uplifted simultaneously, and a new base level for the channel is imposed that is both laterally coincident with the imposed new sea cliff edge and at the altitude of the associated sea level highstand. The magnitude of uplift at the time of placement of each terrace corresponds to the measured differences between inner edge altitudes for the five emergent terraces. Cliff heights are set by the inner edge altitudes of the newly emerged terrace, the known slope of the emergent platform, and the measured width of the intervening platform tread. A regolith (recessional marine sands) of uniform thickness is assumed to cover the newly emergent platform.

#### Bedrock Weathering Rule

The bedrock weathering rate is taken to be a function of local regolith depth. We impose a weathering rate that decreases exponentially with regolith depth, the highest rate occurring on a bare rock surface [Ahnert, 1970; Anderson and Humphrey, 1989]. The exponential decay is scaled by a characteristic regolith depth where the weathering rate is  $(1/e)$

of the bare bedrock rate  $W_0$ . Realistically, the weathering rate is likely to be greatest where bedrock is thinly mantled, rather than bare [Gilbert, 1877; Ahnert, 1970]; we nonetheless proceed with the simplest model, hoping to capture the essence of the problem, that the dependence on regolith thickness be strong. Therefore

$$w(s) = w_0 \exp\left(-\frac{s}{s_*}\right) \quad (1)$$

where  $w(s)$  is weathering rate as a function of depth [L/T],  $w_0$  is surface weathering rate when  $s=0$ , [L/T],  $s$  is regolith thickness [L], and  $s_*$  is characteristic regolith thickness scale [L]. As discussed above, weathering is negligible at typical terrace cover deposit depths of 3-5 m, and the majority of the clay production within the soil profile takes place within the top 0.5 m, motivating an initial choice of  $s_* \leq 0.6$  m.

We estimated the bare bedrock weathering rate  $w_0$  by assuming that the height from the youngest paleosea cliff midpoint to the extrapolated initial position of the wavecut platform surface above it was a crude measure of the vertical loss of bedrock since abandonment of the cliff by the sea. The bedrock at this point is most likely to have had minimal regolith cover throughout its history, as it was at the edge of the cliff, in a zone of consistently high negative curvature. Weathering rates calculated in this manner range from 0.50-0.05 m kyr<sup>-1</sup>.

### Hillslope Process Rules

Conservation of mass in the hillslope system leads to the erosion equation, which describes the change of elevation at a point as a function of time.

$$\frac{\partial z}{\partial t} = -\frac{\partial Q_x}{\partial x} \quad (2)$$

where  $Q_x$  is the volumetric transport rate in the  $x$  direction, or specific discharge of sediment [V/LT]. If the transport rate of material downslope is linearly proportional to local slope: i.e., in the one-dimensional case,

$$Q_x = -C \frac{\partial z}{\partial x} \quad (3)$$

where  $C$  reflects transport efficiency, then the diffusion equation results:

$$\frac{\partial z}{\partial t} = -\frac{\partial Q_x}{\partial x} = -\frac{\partial\left(-C \frac{\partial z}{\partial x}\right)}{\partial x} = \kappa \frac{\partial^2 z}{\partial x^2}$$

or, in two dimensions,

$$\frac{\partial z}{\partial t} = \kappa \left[ \frac{\partial^2 z}{\partial x^2} + \frac{\partial^2 z}{\partial y^2} \right] \quad (4)$$

The coefficient,  $C$ , is now identified as  $\kappa$  = hillslope diffusivity [L<sup>2</sup>/T], and is assumed to be spatially uniform. This relationship precludes processes that are dependent on distance from the drainage divide, such as slope wash [Carson

and Kirkby, 1972], or landsliding processes, which would entail a threshold slope angle.

Earlier workers have applied analytical and numerical solutions of the diffusion equation to describe the evolution of various hillslope geometries [e.g., Cullings, 1960; Nash, 1980; Hanks et al., 1984; Andrews and Hanks, 1985]. From equation (4) we see that a purely diffusive model redistributes material according to the diffusivity and the local topographic curvature. Areas with high negative curvature will be smoothed by the transport of material away from the region. The evolution of fault scarps in unconsolidated lake shore sediments exemplifies the type of landscape adequately described by pure diffusion, the processes being rain splash, creep, etc. [e.g., Nash, 1980]. Slope aspect can also play a role [Pierce and Colman, 1986] through altering both process types and rates.

Pure diffusion does not capture fully the evolution of topography in the face of a limited supply of mobile material [Anderson and Humphrey, 1989]. In the case of bedrock scarps, the material to be transported must first be produced in situ by weathering. Hanks et al. [1984] used a pure diffusion model to describe the Santa Cruz marine terrace sequence. Evolution of a purely diffusive landscape will produce a symmetrical profile about the slope inflection point [e.g., Hanks et al., 1984; Andrews and Hanks, 1985]. In contrast, the surveyed marine terrace profiles show an asymmetry about the inflection point and the edges of paleocliffs are clearly only thinly mantled by regolith (Figures 4 and 5). Such profile shapes are to be expected in a weathering-limited diffusive landscape [Anderson and Humphrey, 1989].

In our model, erosion in a particular time step may not exceed the amount of transportable material available at that point. We must therefore explicitly track both the surface topography and the interface of the regolith and the bedrock. We slightly modify the diffusion algorithm typically used in hillslope models by modifying the local hillslope diffusivity. We define a transport scaling depth  $z_*$  corresponding to the estimated depth of the layer involved in transport. For a regolith thickness greater than  $z_*$ , the diffusivity is not affected by the regolith depth, whereas for regolith thicknesses less than  $z_*$ , the diffusivity becomes

$$\kappa_{\text{lim}} = \kappa \left( \frac{s}{z_*} \right) \quad (5)$$

where  $\kappa$  is maximum hillslope diffusivity [L<sup>2</sup>/T],  $\kappa_{\text{lim}}$  is weathering-limited diffusivity [L<sup>2</sup>/T],  $z_*$  is base of the transport layer [L], and  $s$  is local regolith depth, [L]. Note that this brings the transport rate smoothly to zero as the regolith thickness vanishes.

### Stream Process Rules

The energy per time available to erode a stream channel is defined as the stream power [e.g., Leopold et al. 1964; Bull, 1979]. Stream power is proportional to the product of local channel slope and local drainage area [e.g., Chappell, 1974; Hirano, 1976; Howard and Kerby, 1983; Willgoose et al., 1991; Seidl and Dietrich, 1992], where the drainage area above a point in the channel is a surrogate for water discharge [Hack, 1957]. Howard et al. [this issue] propose a generalized rule for incision in bedrock channels:

$$\frac{\partial z}{\partial t} = -\alpha A^n \left( \frac{\partial z}{\partial x} \right)^m \quad (6)$$

where  $A$  is drainage basin area above a position in the channel [ $L^2$ ],  $\alpha$  is the constant of proportionality representing incision efficiency [ $1/LT$ ],  $z$  is elevation of the channel,  $x$  is upstream distance, and the exponents  $m$  and  $n$  are determined empirically. *Seidl and Dietrich* [1992] argue through Playfair's law applied to measured channel profiles in Oregon that the exponents  $m$  and  $n$  should both be 1. Following this lead, the first term in our stream incision rule is

$$\frac{\partial z}{\partial t} = -\alpha A \frac{\partial z}{\partial x} \quad (7)$$

The relative efficiency of the channel incision process  $\alpha$  will be a function of lithology (the efficiency of the conversion of stream power to lowering of the bed) and of climate, which will determine the distribution of stream discharge events that supply the power. For situations in which the drainage area may be taken to be a constant within the reach of concern, which we argue is the case in the terraced fringe of these coastal basins, the solution to this equation is a migrating waveform of constant shape, i.e.,

$$z(x) = z(x-vt) \quad (8)$$

where  $v$  is the migration speed of the knickpoint or convexity. It may be shown that  $v = \alpha A$ . This term of the stream rule therefore describes the upstream advection of a self-similar knickpoint profile (Figure 7c). Convexities in channels with large drainage areas and weak lithologies will migrate fastest.

We also observed that channel convexities appear to relax with distance upchannel, and hence with age (Figure 7d), prompting the inclusion of a diffusive term:

$$\frac{\partial z}{\partial t} = \kappa_c \left( \frac{\partial^2 z}{\partial x^2} \right) \quad (9)$$

*Begin* [1988] used such a diffusive description to model the reequilibration of alluvial channels following a drop in base level. Our final stream rule therefore includes two terms to describe convexity advection and diffusion:

$$\frac{\partial z}{\partial t} = -\alpha A \frac{\partial z}{\partial x} + \kappa_c \left( \frac{\partial^2 z}{\partial x^2} \right) \quad (10)$$

where the rate-controlling coefficients  $\alpha$  and  $\kappa_c$  will be determined through modeling of the stream profiles.

In our calculations, the drainage area  $A$  is held constant for two related reasons: (1) discharge for the modeled stream arises relatively far from the terrace sequence (in this sense the stream may be considered exogenous) and (2) the channel length through the marine terrace sequence is short relative to the total stream length. The incision constant  $\alpha$  and the diffusivity  $\kappa_c$  are held spatially uniform and temporally steady within each model run.

### Numerical Model and Model Calibration

The rules described above are embedded in a transient, two-dimensional finite difference model [Rosenbloom, 1992]. The problem domain is a rectangle bounded on one side by a stream. Grid spacing is uniform in  $x$  and  $y$ . The initial

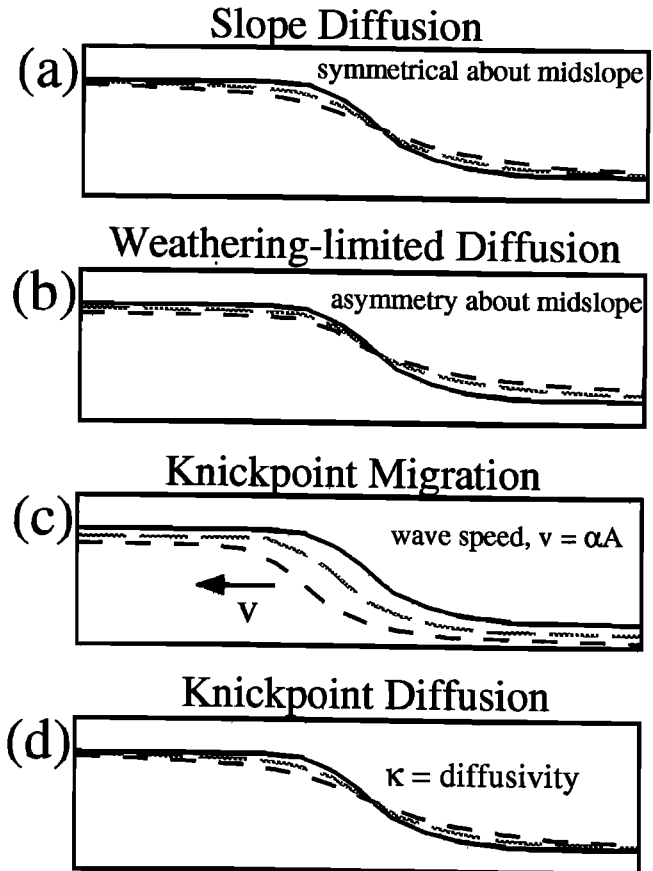


**Figure 7.** Schematic illustration of possible slope evolution (Figures 7a and 7b) and stream profile evolution (Figures 7c and 7d) given initial conditions as shown in the heavy lines. (a) Symmetrical decay would result from simple linear diffusion, controlled by a diffusion coefficient,  $\kappa$ . (b) Asymmetrical decay would result from inclusion of bedrock weathering and diffusive transport. (c) Upstream advection of channel convexities results from application of the stream power rule (see text) the celerity of the knickpoint being controlled by the product of the drainage area  $A$  with the incision efficiency,  $\alpha$ . (d) For generality, we assume that a knickpoint may also simply diffuse, lowering in slope through time without propagating, the decay rate set by a channel diffusivity  $\kappa$ .

condition is a tilted planar slab into which the channel is initially incised by an arbitrary 2 m. In the first time step, the first sea cliff and subjacent wavecut platform are notched into the landscape, the base of the sea cliff becoming the new base level for the stream.

Model results were compared with survey profiles using the reduced  $\chi^2$  statistic [Bevington, 1969]:

$$\frac{\chi^2}{\nu} = \left( \frac{1}{N-n-1} \right) \sum_{i=1}^N \left\{ \frac{1}{\sigma_i^2} [z_i - z(x_i)]^2 \right\} \quad (11)$$

where  $\sigma_i$  is estimated error ( $\pm 3.0$  m),  $z_i$  is profile survey data,  $z(x_i)$  are computed model results, and  $\nu$  is the number of degrees of freedom:  $\nu = N - n - 1$ , where  $N$  is number of data points and  $n$  is number of model parameters (4). A reduced  $\chi^2 < 1$  indicates a very close fit between model and data. Field profile data points were assigned to those of the model by

linear interpolation between model nodes. For each of the two surveyed profiles, the model strategy consisted of a grid search through parameter space in which production of a model is accompanied by calculation of the goodness of fit to the field data, followed by a change in one model parameter. The sensitivity of the model to the full range of plausible parameter combinations was determined. We report below both the favored solutions and the degree to which the model is sensitive to the various geomorphic parameters involved.

### Hillslope Results and Discussion

In Figure 8 we show the profiles of the paleocliffs and intervening terrace risers at the end of the simulation that produced the lowest reduced  $\chi^2$ . Hillslope diffusivities of order  $10 \text{ m}^2 \text{ kyr}^{-1}$ , a bare bedrock weathering rate of  $0.3 \text{ m kyr}^{-1}$ , and a scaling depth of  $0.5 \text{ m}$  for the rate at which weathering decays with regolith thickness are favored (Figure 9). As expected, the ancient sea cliff profiles become more rounded with time. The maximum slope diminishes with time, and the products of the cliff decay accumulate at the base of the cliffs as prograding colluvial aprons. Cliffs are asymmetrical, their tops having smaller radii of curvature than their bases. Regolith is thinnest above the midpoint of each cliff, is nearly absent on the youngest emergent cliff top, and increases in minimum thickness with age, in accord with observations depicted in Figure 4.

The model appears to be very sensitive to the hillslope diffusivity, with a narrow range of best fit solutions (Figure 9a). Diffusivities greater than  $40 \text{ m}^2 \text{ kyr}^{-1}$  and less than  $5.0 \text{ m}^2 \text{ kyr}^{-1}$  are definitely rejected as solutions. Using the older terrace ages suggested by *Lajoie et al.* [1986] (Table 1) results in best fitting hillslope diffusivities of  $5 \text{ m}^2 \text{ kyr}^{-1}$  reflecting the longer times over which the hillslope processes have had to operate. The small difference in the  $\chi^2$  ranking of the best fit models using each of these two age assignments does not allow discrimination between the two sets of age assignments.

Not surprisingly, the best fitting diffusivity is similar to the  $11 \text{ m}^2 \text{ kyr}^{-1}$  calculated by *Hanks et al.* [1984] for the same terrace sequence and choice of age assignment. *McKean et al.* [1993], working in clay-rich hillslopes  $100 \text{ km}$  inland east of Berkeley, California, have shown through completely different methods based upon  $^{10}\text{Be}$  concentration patterns that soil creep can indeed be shown to be dependent linearly upon local slope, and that the diffusion coefficient in that landscape was about  $40 \text{ m}^2 \text{ kyr}^{-1}$ . That these slopes would diffuse more rapidly than those dominated by the coarser textured regolith in motion in the Santa Cruz terraces is to be expected. *McKean et al.* [1993] cite earlier work in coarser textured hillslopes of the western coast ranges with diffusivities of  $4.2 \pm 2.3 \text{ m}^2 \text{ kyr}^{-1}$  [*Reneau et al.*, 1989], the mean of which is near the lower bound of our best fitting diffusivities. We do note that these rates fit better the second (older) age assignment suite, although the large uncertainty in the diffusivities reported by *Reneau et al.* [1989], and the undoubted difference in process types and the intensities along the coast ranges conspire to eliminate a match of best fitting diffusivities as a means of discriminating between age assignments.

We have argued that burrowing animals appear to be responsible for the primary sediment transport on the hillslopes and have shown that such transport should be diffusive [see *Rosenbloom*, 1992]. Preliminary diffusivities

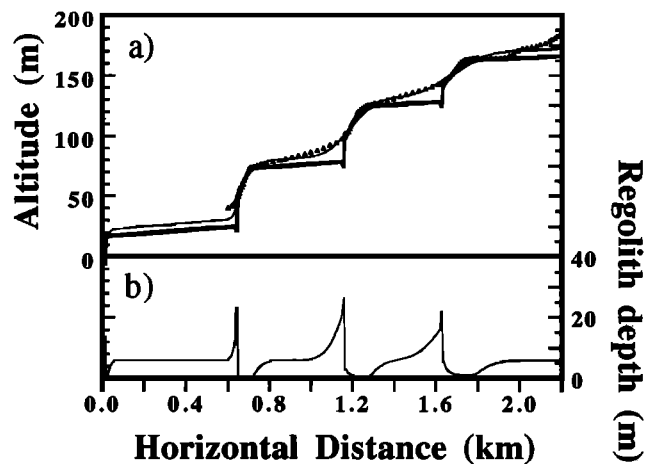
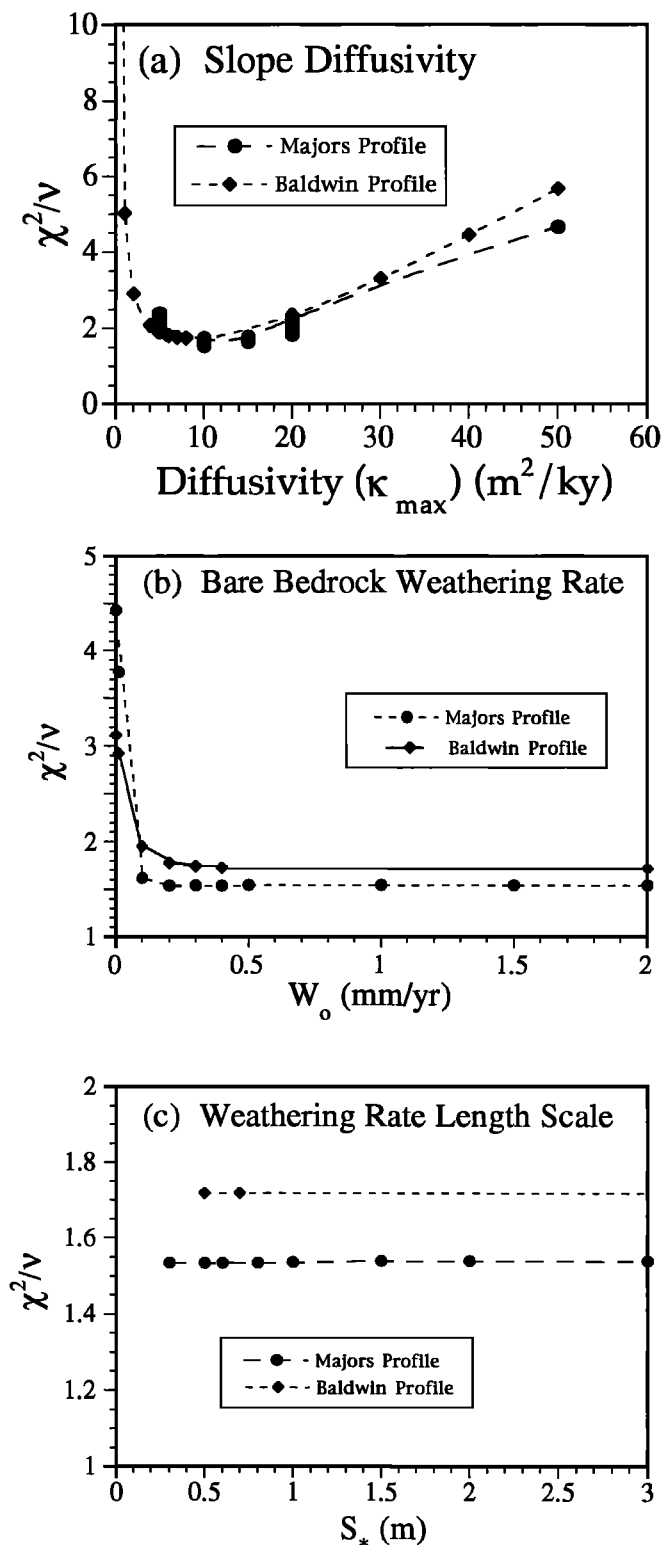


Figure 8. (a) Example of modeled terrace surface profiles shown with the surveyed data (Majors profile, Figures 1, 5, and 6). Wavecut platforms are shown as inserted into the model at the distances required by the locations of the paleocliffs and the times prescribed by the assumed ages of the sea's abandonment of the inner edges (Figure 5). The intervening wedge of material is a combination of original marine terrace deposits (here assumed to be uniformly  $6 \text{ m}$  thick upon retreat of the sea), and colluvium derived from the decay of the sea cliff backing any particular terrace. (b) The regolith depth as a function of position. Note the spike associated with the base of the cliff and the taper that grows through time. Regolith is absent on the bedrock-dominated edge of the first cliff but has a finite but low depth on the upper edges of older cliffs. The terrace surfaces of old or narrow platforms will dip significantly more toward the sea than will younger and broader surfaces, suggesting that caution is warranted in interpreting dips of these surfaces as tilt of the original platforms.

of  $0.54\text{--}2.2 \text{ m}^2 \text{ kyr}^{-1}$  and consequent sediment transport rates of  $0.08\text{--}33 \text{ m}^3 \text{ m}^{-1} \text{ kyr}^{-1}$ , calculated from field measurements of burrowing activity, agree well with results from previous studies [*Black and Montgomery*, 1991; *Lehre*, 1982, 1987]. However, the diffusivities calibrated from the terrace sequence modeling are roughly an order of magnitude greater than these preliminary field data suggest. The discrepancy may be due to (1) poor sampling of burrowing activity in our field area; (2) variable activity through time; (3) a poor estimate of the time interval represented by "fresh" debris; and (4) hillslope transport processes we have not considered. Additional investigation of all parameters influencing burrowing activity is warranted.

Best fitting bedrock weathering rates  $w_0$  are  $0.2\text{--}0.3 \text{ m kyr}^{-1}$  (Figure 9b). The model is very insensitive to bare bedrock weathering rates greater than this but definitely rejects bedrock weathering rates less than  $0.1 \text{ m kyr}^{-1}$ . Significantly, this is well within the range of estimates of soil production rates in a shale-dominated Black Diamond Park landscape  $100 \text{ km}$  to the east, where profiles of atmospherically produced  $^{10}\text{Be}$  have been used to calculate soil production rates of order  $0.25 \text{ m kyr}^{-1}$  [*Monaghan et al.*, 1992] and  $0.26\text{--}0.07 \text{ m kyr}^{-1}$  [*McKean et al.*, 1993]. Recall, however, that  $w_0$  is the maximum rate to be expected in our landscape, as it represents regolith production from bare bedrock. The Black Diamond Park site is clothed uniformly in roughly  $0.5 \text{ m}$  of soil and is



**Figure 9.** Sensitivity analyses of the parameters controlling the shapes of the model hillslope profiles. Tests used the reduced  $\chi^2$  statistic relating model calculations to real data (see text). (a) The most highly selected parameter (a) is the hillslope diffusivity  $\kappa$ . For both surveyed profiles the minimum  $\chi^2$  corresponds to  $\kappa = 10 \text{ m}^2 \text{ kyr}^{-1}$ . (b) Sensitivities of the weathering rate on bare bedrock and (c) of the rate at which it falls off with regolith cover thickness show less pronounced minima for the range of these parameters tested.

chosen particularly because the assumption of steady state form, including soil thickness, could be justified.

The best fitting scaling depth  $z_0$  of 0.5 m for decay of the weathering rate with regolith depth (Figure 9c) agrees well with the observations of local terrace soils in which a prominent clay horizon is found at roughly 0.4 m and with the lack of significant weathering of underlying pholad-bored bedrock wavecut platforms (Figure 4). The correspondence between the two independent results strengthens our initial choice of a characteristic scaling depth of  $<0.6 \text{ m}$ . Model sensitivity to this scaling depth, however, was very low (note scale on Figure 9c), with a narrow range of variation. We therefore calculate a regolith production rate beneath 0.5 m of soil to be roughly  $w_0/e$ , or  $0.1 \text{ m kyr}^{-1}$ , or roughly 2 times that at the Black Diamond site. Although the precipitation at the Santa Cruz site is twice that at the more inland site, the siliceous Santa Cruz mudstone appears to weather less rapidly than the Eocene marine shale bedrock at the Black Diamond Park site.

Coast-parallel hillslope profiles taken perpendicular to the incising streams show a characteristic parallel retreat (Figure 10). Near-channel slopes cut into bedrock are steep and straight and support little regolith. The weathering rates are consequently high, and nearly uniform, resulting in slope-parallel retreat, in places due to mass wasting processes. The crests of these hillslopes, at their intersection with the terrace flats, are diffused, pulling terrace cover sediments down over the slope toward the stream channel. The process appears to be regulated by the parallel-retreating basal slopes. The widths of the valleys containing these channels increases with the age of the adjacent terrace surface.

We note in passing that in the particular terrace profile modeled, the relatively narrow Wilder terrace is entirely blanketed by the colluvial apron prograding from the decaying sea cliff at its back edge. We note that by assuming that the wavecut platform is parallel to the minimum slope of the terrace surface, one would overestimate the slope of the wavecut platform beneath the cover. This has led earlier workers [Bradley and Griggs, 1976] to postulate that the older platforms dip more steeply offshore than the younger platforms, reflecting tectonic tilt through time. This is an effect of the progradation of the colluvial apron, an effect greatest on narrow platforms; there is little evidence of coast-normal tectonic tilting.

### Stream Results and Discussion

The model is relatively insensitive to channel diffusivity within the range  $10\text{--}500 \text{ m}^2 \text{ kyr}^{-1}$ , while diffusivities greater than  $500 \text{ m}^2 \text{ kyr}^{-1}$  are clearly ruled out. As seen in Figure 11, the model is very sensitive to the incision efficiency,  $\alpha$ , which is constrained to lie between  $5 \times 10^{-7}$  and  $7 \times 10^{-7} \text{ m}^{-1} \text{ kyr}^{-1}$ .

Weathering rate on bare bedrock appears to be roughly  $0.2\text{--}0.3 \text{ mm yr}^{-1}$ , with lower rates effectively ruled out. The selected length scale appears to be of the order of  $0.5\text{--}0.6 \text{ m}$ , although here there is little sensitivity. Field data rule out scales much greater than this. Twice the  $0.5 \text{ m}$  depth (by which depth weathering rates would have fallen to a tenth of the bare bedrock rate) corresponds well with the depth of significant soil development on the older terraces (see Figure 5).

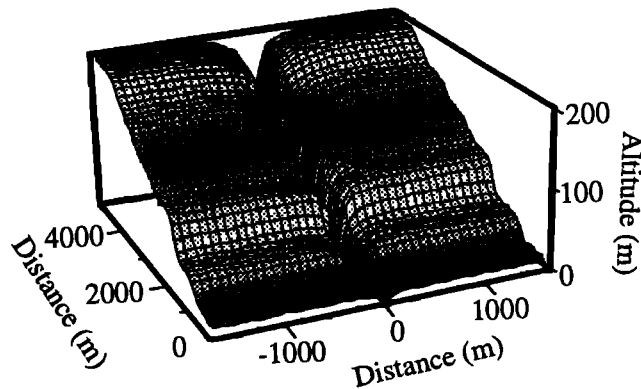


**Figure 10.** Perspective plot of the three-dimensional model landscape. Note the relatively straight-sided walls of the stream valley below diffused edges. The older terrace platforms are being attacked from all sides, the paleoclimbs at their backs and fronts decaying, while the channels that are progressively more deeply incised beside them cause lateral encroachment of the channel valley walls into the terrace platform. Nonetheless, platforms of order several hundred thousand years are clearly preserved well in this landscape, given the low hillslope diffusivities and weathering rates.

Larger values of  $\alpha$  drive the channel convexity upstream and downward too rapidly, while smaller values leave the channel well above the measured profile. We have not attempted to model the highest channel convexity; we have no constraint on the appropriate initial conditions (inner edge location) associated with an older terrace.

The other two major convexities are evident in the model, although even the best model fails to reproduce accurately the knickpoint curvatures and lateral positions of these convexities simultaneously. The lowest model knickpoint is

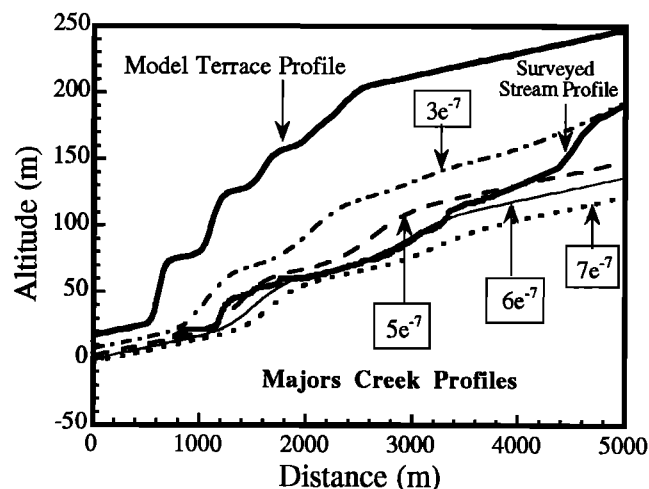


**Figure 11.** Model stream results, with stream profile data (heavy line) for comparison. Four model profiles are shown using four values of the incision efficiency factor  $\alpha$  in  $\text{m}^{-1} \text{kyr}^{-1}$ . Drainage area is assumed not to vary through the reach of concern. The locations of the first and second convexities are well simulated using roughly  $\alpha = 6 \times 10^{-7} \text{m}^{-1} \text{kyr}^{-1}$ . The third convexity is not modeled because the terrace to which it would correspond is not used in the calculation. The best fitting modeled terrace surface profile is shown for comparison.

not as sharp as the measured convexity. Although this presumably reflects physics of the incision process not faithfully mimicked by the stream incision rule, we emphasize that the essence of the complicated channel profile is captured.

A complex interaction between sea level fluctuation, sea cliff retreat, tectonic uplift, and stream incision controls the likelihood of the formation of channel convexities. At glacially induced sea level lowstands, coastal streams drain to the new base level more than 4 km offshore and 120-150 m below present sea level and begin to incise the recently abandoned wavecut platform. The longer sea level remains low, the deeper the incision across the exposed wavecut platform. In the following interglacial period, a new sea cliff forms at an altitude relative to the last-abandoned sea cliff that is a function of the difference in altitude between the two highstands and the length of time between successive highstands. The time interval determines the magnitude of intervening tectonic uplift. The retreat of the active sea cliff will continually reduce the breadth of the most recently emergent terrace. A new wavecut platform will be abraded, with an offshore 1-2° profile. As the highstand is approached, the advancing sea cliff will increase in height as it etches horizontally into a landscape with mean slopes much greater than 1-2°. A channel convexity occurs only if the advancing base of the active sea cliff (the inner edge) intersects the incised stream channel. Remnants of bedrock channels incised into the subaerially exposed wavecut platform during the lowstand may be preserved if in the subsequent highstand the sea cliff fails to intersect the incised channel. In this latter case, the bedrock channel will be drowned and the mouth of the stream will be alluviated.

Cast more formally [see *Rosenbloom, 1992*], formation of a channel convexity requires that at the site of the future inner edge, the stream incision between sea level highstands must be less than the sum of the initial depth and the tectonic uplift at the same site in the same time interval. Using reasonable parameters for the Santa Cruz coast (uplift rate of  $0.3 \text{ m kyr}^{-1}$ , time between highstands of 100kyr, initial depth of the platform at the future location of an inner edge of 5 m (wavecut platform angle 1°, emergent platform width 300 m)), we find that an average channel incision rate of  $< 0.25 \text{ m kyr}^{-1}$  is required for the formation of channel convexities. Referring to the stream incision rule (equation (10)), a low incision efficiency and a small drainage basin area will lead to low mean rates of channel incision and more probable formation of a channel convexity. In general, high rates of tectonic uplift, shallow terrace slopes, narrow emergent terrace widths, lower sea level highstands, and shorter glacial periods (lowstands) are more likely to result in convexities. In the study area, with drainage basins of order  $10 \text{ km}^2$ , and channel slopes across the wavecut platform of 1-2°, the required incision rate for channel convexity formation implies an incision efficiency  $\alpha$  of order  $7 \times 10^{-7} \text{ m kyr}^{-1}$ , in accord with the model findings.

It is clear from the alluviated mouths of streams such as Majors and Laguna Creeks and from the submerged sand-filled channels crossing the modern wavecut platform that several of these coastal streams were powerful enough to incise both the Highway 1 platform and the modern wavecut platform during the last sea level lowstand. Creation of a channel convexity during the present sea level highstand will require landward retreat of the present cliffs by many hundred meters.

Channel convexities of the intermediate size, order  $10 \text{ km}^2$

basin area, throughflowing streams along this section of the coast reflect variable response to the complex base level history to which they have all been subjected in the late Pleistocene. That the stream power is not uniform from channel to channel, due to even small differences in basin drainage area, is reflected in the variable numbers and altitudes of the convexities preserved (Figure 6). Large streams outside of the study area do not have prominent convexities, implying higher mean incision rates commensurate with their larger basin areas.

## Conclusions

We are encouraged that the best fitting hillslope diffusivity and bedrock regolith production rates obtained in our study are comparable to diffusivities and regolith production rates measured in nearby central California using completely independent methods [McKean *et al.*, 1993]. The simple linear diffusion model is adequate to explain the details of the hillslope profiles, including, importantly, the regolith depth; it does not require the adoption of nonlinear hillslope diffusion rules [Andrews and Bucknam, 1987].

That the channel morphology is less well captured by the model than the hillslopes reflects the crudeness of the stream rule and the more complicated forcing history to which stream channels are subjected. Nonetheless, the convexity-forming process has been identified and explains well (1) the presence or absence of convexities in channels draining basins of differing size, (2) the stream-to-stream variability in altitudes of existing convexities, and (3) the presence of both drowned channel mouths and sand-filled channels crossing the modern wavecut platform.

The channels serve to illustrate the imperfection of many of these geomorphic features for deducing sea level and tectonic history along this and other coasts. Terrace platforms may be entirely removed by landward advance of a subsequent lower inner edge, making the terrace record variably complete along a particular coastline, largely at the whim of the long-term cliff retreat efficiency. This in turn will initiate channel convexities of differing magnitudes in streams draining the coastal landmass, the subsequent migration and incision rates of which will be determined by the size of the drainage basin. It is therefore no wonder that both the stream and terrace profiles vary significantly along a coast, even if the uplift rates were uniform.

The modeling illustrated here could be fruitfully extended along several lines. The wavecut platform and sea cliff insertion rule in the present model is crude; the inner edges and associated sea cliffs are instantaneously placed in the landscape in their final position at the time of the corresponding sea level highstand. At the next time step, base level is dropped well down the associated wavecut platform to await the time of the next sea level highstand. The model would more faithfully mimic the geomorphic evolution of the landscape if a more continuous sea level and cliff retreat history were imposed. Such a history would require a rule connecting cliff recession rate to local lithology, the local wave energy field, the evolving cliff height, and the relative rate of sea level rise and would therefore require knowledge of sea level history throughout the past several hundred thousand years. We know relatively well the ages of the highstands but have information about the rate of approach to a highstand

from only the last deglaciation [Fairbanks, 1989; Bard *et al.*, 1990]. The duration of the highstands is only sketchily known for the last few interglacial periods; they have lasted from several to more than 20 kyr [Rockwell *et al.*, 1992]. Given this, we chose to use the simplest possible cliff and platform insertion rule. Associated error in the hillslope results arises principally through uncertainty in the time of cliff abandonment, which occurs at the end of the sea level highstand. Since the duration of the highstands is short compared to the interval between highstands, the essence of the channel base level history is captured by the model.

In a related issue, no alluvial deposition is allowed in the current model. As this occurs naturally only during sea level highstands, the duration of the highstand should play a role in determining the total accumulation of alluvium. The mouth of the bedrock channel protected by alluvium will clearly not be eroded until the alluvium is extracted upon sea level fall. If deposition were implemented, one could mimic the alluviation of channel mouths and the preservation of these deposits as fill terraces seen on more rapidly uplifting coastlines (e.g., near the Mendocino triple junction, California [Merritts *et al.*, this issue]).

In the present model we assume a steady geomorphic forcing. While this assumption may be justified to first order in our study area, the glacial climates were undoubtedly characterized by an altered frequency of high-intensity storm events. A greater runoff would increase stream power (i.e., alter the constant in the stream rule) and the consequent incision rate. Such an asymmetry in the geomorphic forcing between glacial and interglacial times could be quite pronounced in some settings and could leave a very different characteristic landscape.

Even in its present state, however, this exercise illustrates the utility of geomorphic data sets that include not only the relevant surface morphology but also information about the deposit geometries above bedrock in both channels and hillslopes. Such data can be used rigorously in the testing of landscape evolution models, especially when independent evidence allows timing and initial conditions in the landscape to be known.

## Notation

$A$	=	local drainage basin area [ $L^2$ ]
$\alpha$	=	channel incision efficiency [ $1/LT$ ]
$C$	=	hillslope transport efficiency [ $V/LT$ ]
$\chi^2$	=	chi-squared statistic
$\kappa$	=	hillslope diffusivity [ $L^2/T$ ]
$\kappa_c$	=	stream channel diffusivity [ $L^2/T$ ]
$\kappa_{lim}$	=	weathering-limited diffusivity ( $s < z_s$ ) [ $L^2/T$ ]
$m, n$	=	empirically derived exponents in stream incision expression
$N$	=	number of data points
$n$	=	number of parameters being fit
$\nu$	=	degrees of freedom = $N - n - 1$
$L$	=	distance of stream from the terrace midpoint [ $L$ ]
$Q_x$	=	volumetric transport rate in the $x$ direction [ $V/LT$ ]
$s$	=	local regolith thickness [ $L$ ]
$s_c$	=	characteristic weathering length scale [ $L$ ]
$\sigma_1$	=	estimated error [ $L$ ]
$t$	=	time [ $T$ , (ky)]
$u_0$	=	surface regolith velocity [ $L/T$ ]
$v$	=	migration speed of channel convexity [ $L/T$ ]

- w(s) = weathering rate as a function of regolith depth [L/T]  
 $w_0$  = bare bedrock weathering rate (when  $s = 0$ ) [L/T]  
 $x$  = upstream distance from present sea cliff [L]  
 $z(x_i)$  = computed model elevation [L]  
 $z_i$  = profile survey altitudes [L]  
 $z_0$  = base of active regolith layer [L]

**Acknowledgments.** Acknowledgment is made to the donors of the Petroleum Research Fund, administered by the American Chemical Society, for the support of this research. We appreciate the help of J. Stock and M. Schwartz in construction of hand level surveys and Jim Tait for sharing recent sidescan sonar data. Careful reviews by R. Burgmann, D. Merritts, and K. Vincent, greatly improved the manuscript.

## References

- Ahnert, F., Brief description of a comprehensive three-dimensional process-response model of landform development, *Z. Geomorphol., Suppl.*, 24, 11-22, 1970.
- Alexander, C. S., The marine and stream terraces of the Capitola-Watsonville area, *Univ. Calif. Publ. Geog.*, 10, 1-44, 1953.
- Anderson, P. M. et al., Climatic changes of the last 18,000 years; Observations and model simulations, *Science*, 241, 1043-1052, 1988.
- Anderson, R. S., Evolution of the northern Santa Cruz Mountains by advection of crust past a San Andreas fault bend, *Science*, 249, 397-401, 1990.
- Anderson, R. S., Evolution of the Santa Cruz Mountains, California, through tectonic growth and geomorphic decay. *J. Geophys. Res.*, this issue.
- Anderson, R. S., and N. F. Humphrey, Interaction of weathering and transport processes in the evolution of arid landscapes, in *Quantitative Dynamic Stratigraphy*, edited by T. A. Cross, pp. 349-361, Prentice-Hall, Englewood Cliffs, N.J., 1989.
- Anderson, R. S., and K. M. Menking, The Santa Cruz Marine Terraces: Evidence for two coseismic uplift mechanisms, *Geol. Soc. Am. Bull.*, 106, 649-664, 1994.
- Andrews, D. J., and R. C. Bucknam, Fitting degradation of shoreline scarps by a nonlinear diffusion model, *J. Geophys. Res.*, 92, 12,857-12,867, 1987.
- Andrews, D. J., and T. C. Hanks, Scarp degraded by linear diffusion: Inverse solution for age, *J. Geophys. Res.*, 90, 10,193-10,208, 1985.
- Bard, E., B. Hamelin, and R.G. Fairbanks, U-Th ages obtained by mass spectrometry in corals from Barbados: sea level during the past 130,000 years, *Nature*, 346, 456-458, 1990.
- Begin, Z. B., Application of a diffusion-erosion model to alluvial channels which degrade due to base-level lowering, *Earth Surf. Processes Landforms*, 13, 487-500, 1988.
- Best, T.C., and G. B. Griggs, A sediment budget for the Santa Cruz littoral cell, California, in *From Shoreline to Abyss, Spec. Publ., Soc. Econ. Paleontol. Mineral.*, 46, 35-50, 1991.
- Bevington, P. R., *Data Reduction and Error Analysis for the Physical Sciences*, 336 pp, McGraw-Hill, New York, 1969.
- Black, T. A., and D. R. Montgomery, Sediment transport by burrowing mammals, Marin County, California, *Earth Surf. Processes Landforms*, 16, 163-172, 1991.
- Brabb, E. E., Geologic map of Santa Cruz County, California, scale 1:62,500, *U. S. Geol. Surv. map I-1905*, 1989.
- Bradley, W. C., Carbon-14 date for a marine terrace at Santa Cruz, California, *Geol. Soc. Am. Bull.*, 67, 675-677, 1956.
- Bradley, W. C., Origin of marine-terrace deposits in the Santa Cruz area, California, *Geol. Soc. Am. Bull.*, 68, 421-444, 1957.
- Bradley, W. C., Marine terraces on Ben Lomond Mountain, California, in *International Association of Quaternary Research 7th Congress, Guidebook for Field Conference I, Northern Great Basin and California*, edited by C. Wahrhaftig et al., pp. 148-150, Neb. Acad. Sci, Lincoln, Nebraska, 1965.
- Bradley, W. C., and W. O. Addicott, Age of first marine terrace near Santa Cruz, California, *Geol. Soc. Am. Bull.*, 79, 1203-1210, 1968.
- Bradley, W. C. and G. B. Griggs, Form, genesis, and deformation of central California wave-cut platforms, *Geol. Soc. Am. Bull.*, 87, 433-449, 1976.
- Branner, J. C., J. F. Newsom, and R. Arnold, Santa Cruz folio, *U.S. Geol. Surv. Geol. Atlas, Folio 163*, 11 pp., 1909.
- Bull, W. B., Threshold of critical power in streams, *Geol. Soc. Am. Bull.*, 90, 453-464, 1979.
- Carson, M. A., and M. J. Kirkby, *Hillslope Form and Process*, 475 pp., Cambridge University Press, New York, 1972.
- Chappell, J., The geomorphology and evolution of small valleys in dated coral reef terraces, New Guinea, *J. Geol.*, 82, 795-812, 1974.
- Chappell, J. M., A revised sea level record for the last 300,000 years on Papua New Guinea, *Search*, 14, 99-101, 1983.
- Chappell, J. M., and N. J. Shackleton, Oxygen isotopes and sea level, *Nature*, 324, 137, 1986.
- Clark, J. C., Tertiary stratigraphy of the Felton-Santa Cruz area, Santa Cruz Mountains, California, Ph.D. thesis, Stanford Univ., Stanford, Calif., 184 pp., 1966.
- Clark, J. C., Geologic map of the southwestern Santa Cruz Mountains between Afo Nuevo Point and Davenport, California, scale 1:24,000, in *U. S. Geol. Survey Open File Report OF-1970*, 1970.
- Clark, J. C., Stratigraphy, paleontology, and geology of the central Santa Cruz Mountains, California Coast Ranges, *U. S. Geol. Surv. Prof. Pap.*, 1168, 51 pp., 1981.
- Culling, W. E. H., Analytical theory of erosion, *J. Geol.*, 68, 336-344, 1960.
- Culling, W. E. H., Theory of erosion on soil-covered slopes, *J. Geol.*, 73, 230-254, 1965.
- Curtis, G. H., J. F. Evernden, and J. Lipson, Age determination of some granitic rocks in California by the potassium-argon method, *Spec. Rep., Calif. Div. Mines*, 54, 16 pp., 1958.
- Dietrich, W. E., and T. Dunne, Sediment budget for a small catchment in mountainous terrain, *Z. Geomorphol. Suppl.*, 29, 191-206, 1978.
- Fairbanks, R. G., A 17,000-year glacio-eustatic sea level record: Influence of glacial melting rates on the Younger Dryas event and deep-ocean circulation, *Nature*, 342, 637-642, 1989.
- Gibbons, A. B., J. D. Megeath, and K. L. Pierce, Probability of moraine survival in a succession of glacial advances, *Geology*, 12, 327-330, 1984.
- Gilbert, G. K., Report on the geology of the Henry Mountains, Washington, U.S. Government Printing Office, Washington, D.C., 1877.
- Griggs, G. B., and R. E. Johnson, Erosional processes and cliff retreat along the northern Santa Cruz County Coastline, *Calif. Geol.*, 32, 67-76, 1979.
- Gorsline, D. S., G. A. Pao, S. E. Prenskey, and M. Mulhern, High resolution studies of paleo-climatic and paleo-oceanographic history in California Continental Borderland basin sediments, *AAPG Bull.*, 60, 675, 1976.
- Hack, J. T., Studies of longitudinal stream profiles in Virginia and Maryland, *U.S. Geol. Surv. Prof. Pap.*, 294-B, 97 pp., 1957.
- Hanks, T. C., R. C. Bucknam, K. R. Lajoie, and R. E. Wallace, Modification of wave-cut and faulting-controlled landforms, *J. Geophys. Res.*, 89, 5771-5790, 1984.
- Hirano, M., Mathematical model and the concept of equilibrium in connection with slope shear ratio, *Z. Geomorphol. Suppl.*, 25, 50-71, 1976.
- Howard, A. D., and G. Kerby, Channel changes in badlands, *Geol. Soc. Am. Bull.*, 94, 739-752, 1983.
- Howard, A.D., M. A. Seidl, and W.E. Dietrich, abstract, Chapman Conference on Tectonics and Topography, Am. Geophys. Union, 1992.
- Jahns, R. H., and D. H. Hamilton, Geology of the Davenport coastal area and the proposed Davenport power plant site area, 33 pp., Pac. Gas and Elec. Co., San Francisco, Calif., 1971.
- James, E.W., Cretaceous metamorphism and plutonism in the Santa

- Cruz Mountains, Salinian block, California, and correlation with the southernmost Sierra Nevada, *Geol. Soc. Am. Bull.*, 104, 1326-1339, 1992.
- Johnson, D. L., The late Quaternary climate of coastal California: Evidence for an ice age refugium, *Quat. Res.*, 8, 154-179, 1977.
- Koons, P. O., The topographic evolution of collisional mountain belts: A numerical look at the Southern Alps, New Zealand, *Am. J. Sci.*, 289, 1041-1069, 1989.
- Lajoie, K. R., G. E. Weber, and J. C. Tinsley, Marine terrace deformation: San Mateo and Santa Cruz Counties, in *Progress Report on the USGS Quaternary Studies in the San Francisco Bay Area, An Informal Collection of Preliminary Papers*, edited by V. A. Frizzell, pp. 100-113, Friends of the Pleistocene, Palo Alto, 1972.
- Lajoie, K. R., J. F. Wehmler, K. A. Kvenvolden, E. Peterson, and R. H. Wright, Correlation of California marine terraces by amino acid stereochemistry, *Geol. Soc. Am. Abstr. Programs*, 7, 338-339, 1975.
- Lajoie, K. R., D. J. Ponti, C. L. Powell II, S. A. Mathieson, A. M. Sarna-Wojcicki, Emergent marine strandlines and associated sediments, coastal California; A record of Quaternary sea level fluctuations, vertical tectonic movements, climatic changes, and coastal processes, in *The Geology of North America, vol. K-2, Quaternary Nonglacial Geology: Conterminous U.S.*, edited by R. B. Morrison, pp. 190-214, 1986.
- Lawson, A. C., The post-Pliocene diastrophism of the coast of southern California, *Bull. Univ. Calif. Dep. Geol. Sci.*, 1, 115-160, 1893.
- Lehre, A. K., Rates of soil creep on colluvium-mantled hillslopes in north-central California: in *Erosion and Sedimentation in the Pacific Rim*, edited by R. L. Beschta, T. Blinn, G. E. Grant, F. J. Swanson, and G. G. Ice, *IAHS Publ.*, 165, 91-100, 1987.
- Leo, G. W., The plutonic and metamorphic rocks of Ben Lomond Mountain, Santa Cruz County, California, *Spec. Pub. Calif. Div. Mines Geol.* 91, 27-43, 1967.
- Leopold, L. B., M. G. Wolman, and J. P. Miller, *Fluvial Processes in Geomorphology*, 522 pp., W. H. Freeman, New York, 1964.
- McKean, J. A., W. E. Dietrich, R. C. Finkel, J. R. Southon, and M. W. Caffee, Quantification of soil production and downslope creep rates from cosmogenic  $^{10}\text{Be}$  accumulations on a hillslope profile, *Geology*, 21, 343-346, 1993.
- Merritts, D. J., K. R. Vincent, and E. E. Wohl, Long river profiles, tectonism, and eustasy: A guide to interpreting fluvial terraces, *J. Geophys. Res.*, this issue.
- Monaghan, M. C., J. McKean, W. Dietrich, and J. Klein,  $^{10}\text{Be}$  chronometry of bedrock to soil conversion rates, *Earth Planet. Sci. Lett.*, 111, 483-492, 1992.
- Nash, D. B., Morphologic dating of degraded normal fault scarps, *J. Geol.*, 88, 353-360, 1980.
- Nishiizumi, K., C. P. Kohl, J. R. Arnold, R. Dorn, J. Klein, D. Fink, R. Middleton, and D. Lal, Role of *in situ* cosmogenic radionuclides  $^{10}\text{Be}$  and  $^{26}\text{Al}$  in the study of diverse geomorphic processes, *Earth Surf. Processes Landforms*, 18, 407-425, 1993.
- Page, B. M., and C. N. Holmes, Geology of the bituminous sandstone deposits near Santa Cruz, Santa Cruz County, California, *U.S. Geol. Surv. Oil Gas Invest. Prelim. Map* 27, 1945.
- Pierce, K. L., and S. M. Colman, Effect of height and orientation (microclimate) on geomorphic degradation rates and processes, late-glacial terrace scarps in central Idaho, *Geol. Soc. Am. Bull.*, 97, 869-885, 1986.
- Porter, S. C., Some geological implications of average Quaternary glacial conditions, *Quaternary Res.*, 32, 245-261, 1989.
- Rantz, S. E., Average annual precipitation and runoff in north coastal California, scale 1:1,000,000, *U.S. Geol. Surv. Hydrologic Atlas* 298, 1968.
- Reneau, S. L., W. E. Dietrich, M. Rubin, D. J. Donahue, and A. J. T. Jull, Analysis of hillslope erosion rates using dated colluvial deposits, *J. Geol.*, 97, 45-63, 1989.
- Rockwell, T., D. R. Muhs, and G. L. Kennedy, Late Quaternary paleosealevel estimates for the west coast of North America based upon coral-dated marine terraces (abstract), *Geol. Soc. N.Z. Misc. Pubs.*, 65A, 47, 1992.
- Rode, K., Geomorphogenie des Ben Lomond (Kalifornien), eine Studie über Terrassenbildung durch marine Abrasion, *Z. Geomorphol.* 5, 16-78, 1930.
- Rosenbloom, N. A., Calibration of coupled channel and hillslope processes in a marine terraced landscape, Santa Cruz, California, M.S. thesis, 126 pp., Univ. of Calif., Santa Cruz, 1992.
- Seidl, M. A., and W. E. Dietrich, The problem of channel incision into bedrock, *Catena, supp.*, 25, 133-151, 1992.
- Sims, J. D., D. P. Adam, and M. J. Rymer, Late Pleistocene stratigraphy and palynology of Clear Lake, in *Research in the Geysers-Clear Lake Geothermal Area, Northern California*, *U.S. Geol. Surv. Prof. Pap.* 1141, edited by R. J. McLaughlin and J. M. Donnelly-Nolan, 219-230, 1981.
- Valensise, G., and S. N. Ward, Long-term uplift of the Santa Cruz coastline in response to repeated earthquakes along the San Andreas fault, *Bull. Seismol. Soc. Am.*, 81, 1694-1704, 1991.
- Verma, V. K., Map parameters for correlation of marine terraces in California, *Geol. Soc. Am. Bull.*, 84, 2737-2742, 1973.
- Weber, G. E., Pleistocene marine terraces and neotectonics of the San Gregorio fault zone, in *Coastal Geologic Hazards and Coastal tTectonics, Northern Monterey Bay and Santa Cruz/San Mateo County Coastlines*, *Association of Engineering Geologists, San Francisco Section, Guidebook*, edited by G. E. Weber and G. B. Griggs, pp. 64-80, San Francisco, 1990.
- Willgoose, G., R. L. Bras, and I. Rodriguez-Iturbe, Results from a new model of river basin evolution, *Earth Surf. Processes Landforms*, 16, 237-254, 1991.
- Wilson, M. E., Shore topography near Davenport, Santa Cruz County, *Calif. Phys. Geogr. Club Bull.*, 1, 11-17, 1907.

R. S. Anderson, Department of Earth Sciences, University of California, Santa Cruz, CA 95064. (e-mail: rsand@bagnold.ucsc.edu)  
 N. A. Rosenbloom, Department of Geological Sciences, University of Colorado, Boulder, CO 80303.

(Received March 29, 1993; revised December 8, 1993; accepted December 28, 1993.)